Measurements of Peroxyacetyl Nitrate at a Background Site in the Pearl River Delta Region: Production Efficiency and Regional Transport

Zheng Xu[1,2], Likun Xue[1,2*], Tao Wang[1,2], Tian Xia[2†], Yuan Gao[2], Peter K.K. Louie[3], Connie W.Y. Luk[3]

[1] *Environment Research Institute, Shandong University, Ji'nan, Shandong, China*
[2] *Department of Civil and Environmental Engineering, Hong Kong Polytechnic University, Hong Kong, China*
[3] *Environmental Protection Department, the Government of Hong Kong Special Administrative Region, Hong Kong, China*

ABSTRACT

Peroxyacetyl nitrate (PAN) is a trace constituent of the atmosphere but plays important roles in air pollution and atmospheric chemistry. To understand the chemical and transport processes of PAN in the Pearl River Delta (PRD) region, measurements of PAN, its precursors and related parameters were made at a regional background site in late summer and late autumn of 2011. Despite the fairly low ambient levels of PAN in general, several photochemical episodes with peak concentrations of PAN and ozone (O_3) as high as 4.86 and 189 ppbv were observed when the region was under influence of a tropical cyclone. PAN showed a seasonal variation with higher levels in autumn than in summer. PAN production efficiency, defined as the amount of PAN formed per unit amount of nitrogen oxides (NO_x) oxidized, was examined for the polluted PRD plumes, which indicated that PAN production accounted for on average approximately one third of the NO_z formation. The photochemical production efficiency of PAN was much lower with respect to that of O_3, suggesting that ~2.9 ppbv of PAN could be produced per formation of 100 ppbv of O_3 in the PRD plumes. Varying air masses including maritime air, regional air masses from the PRD, and continental outflow from eastern China were identified, which showed different chemical signatures in terms of both pollution levels and NO_z budget. The highest abundances of PAN were measured in the PRD air masses, compared to the lowest concentrations in the marine air. Overall, the present study provides some new insights into the photochemical production and regional transport of PAN in the PRD region, where such investigations were very scarce before.

Keywords: Peroxyacetyl nitrate; PAN production efficiency; Regional transport; Pearl River Delta.

INTRODUCTION

Peroxyacetyl nitrate (PAN) is a principal air pollutant in photochemical smog and a key player in atmospheric chemistry. At high concentrations, PAN poses a potential threat to the human health by causing eye irritation and inducing skin cancer, and also affects adversely vegetation and plant (Stephens, 1969). Due to its temperature-dependent lifetimes, PAN can be transported over long distances at low temperature conditions (e.g., in winter or in the free troposphere) and decompose to nitrogen dioxide (NO_2) when entering warm environments (Singh and Salas, 1983).

This process re-distributes nitrogen oxides (NO_x) over a large scale (regionally and even globally) and regulates ozone (O_3) production in both source and remote regions (Penkett and Brice, 1986; Singh *et al.*, 1986). In the troposphere, PAN is produced exclusively from chemical reactions involving NO_x and volatile organic compounds (VOCs) in the presence of sunlight, and hence is a better photochemical indicator than O_3 that can be influenced by downward transport of the stratospheric air (LaFranchi *et al.*, 2009; Zhang *et al.*, 2009a). Given its important roles in air pollution and atmospheric chemistry, PAN has drawn much attention since it was first discovered in the atmosphere of Los Angeles in 1950s (Grosjean, 2003).

Numerous studies have been conducted to characterize the PAN pollution and understand its formation mechanisms and transport behaviors in America, Europe and Japan (Singh and Hanst, 1981; Aneja *et al.*, 1999; Gaffney *et al.*, 1999; Grosjean *et al.*, 2002; Rubio *et al.*, 2004). In recent, several measurement studies have also been carried out in China, over which there is an increasing concern of air quality accompanying its fast economic development (e.g.,

---

† Now at Department of Civil and Environmental Engineering, University of Michigan, USA

* Corresponding author.
 Tel.: +852-2766 6059; Fax: +852-2330 9071
 E-mail address: xuelikun@sdu.edu.cn

in Lanzhou, Zhang *et al.*, 2009a; Beijing, Liu *et al.*, 2010; Zhang *et al.*, 2011; Xue *et al.*, 2014a). The Pearl River Delta region (PRD) including the adjacent Hong Kong is a hot spot of economic development and air pollution in southern China (Zhong *et al.*, 2013). Previous studies have demonstrated the severity of the photochemical smog problem in this region (Zhang *et al.*, 2007; Zhang *et al.*, 2008; Xue *et al.*, 2014b). Despite the large body of research on O_3 processes (Ding *et al.*, 2004; Zhang *et al.*, 2007; Zhang *et al.*, 2008; Zhang *et al.*, 2012; Ling *et al.*, 2014; Xue *et al.*, 2014c), little has been known about the characteristics and processes of PAN in the PRD. To the best of our knowledge, there is only one piece of measurement study that was conducted downwind of Guangzhou city and the data was analyzed to understand the ozone formation (Wang *et al.*, 2010a). More efforts are required for better understanding the PAN pollution and processes in this 'smog' region.

In the present study, field measurements of PAN, its precursors, and related parameters were conducted at a rural coastal site of Hong Kong (Hok Tsui) in summer and autumn of 2011. The site is an ideal regional background station of southern China that is capable of measuring varying air masses, including oceanic air, polluted plumes from the PRD region, and continental outflow from eastern China (Wang *et al.*, 2009), and hence facilitates an investigation of PAN processes in a regional scale. The data were analyzed to understand the temporal variations, photochemical production efficiency, and regional transport of PAN (and related compounds) in southern China. The present study provides some new insights into the photochemical and transport characteristics of PAN in Hong Kong and the PRD region.

EXPERIMENTAL

The field measurements were carried out at the Hong Kong Polytechnic University's atmospheric research station at Hok Tsui (22.22°N, 114.25°E), which is located in the southeastern tip of Hong Kong Island with a 240° sea view from northeast to southwest (see Fig. 1). The station is established on a small cliff with an altitude of around 60 m above sea level. The air flow is mainly driven by the Asian Monsoons. In summer monsoon seasons, the prevailing wind is southerly, bringing fresh marine air to the station; while in winter monsoon seasons, the prevailing wind direction is northeasterly, so the air pollutants from the PRD region and East China can be carried to the site. Thus this site is capable of measuring varying air masses such as marine air, regional plumes from the PRD, and super-regional air masses from eastern China. It should be noted that the emissions from ships passing over the nearby ocean may also affect the site occasionally. The station has been used as a regional background site in many previous studies, which can be referred for detailed description of the site (Wang *et al.*, 2001). The present study consisted of two separate campaigns, which took place from August 19th to September 16th 2011 and from November 09th to December 05th 2011, respectively.

PAN, O_3, NO, NO_2, NO_y, CO, non-methane hydrocarbons (NMHCs) and meteorological parameters were continuously measured during the campaigns. PAN was measured by using a commercially available automatic instrument together with a calibration unit. The analyzing process is based on gas chromatographic (GC) separation coupled with electron capture detection, as illustrated by Schrimpf *et al.* (1995). The instrument was calibrated weekly using the stable flow of air containing pre-determined PAN concentrations produced by the calibration unit. PAN was synthesized by reactions of known concentrations of NO with excess acetone in the presence of ultra-pure air with a penray lamp. The produced PAN was then diluted to the desired concentration by mixing with the synthetic zero air. The sensitivity of analyzer can be determined from the slope of concentration versus signal, and was found to be stable throughout the campaigns. The linearity of analyzer was also evaluated by performing multi-point calibrations before and after the campaigns. This analyzer has been successfully utilized in our previous studies, from which detailed descriptions of instrument and measurement protocols can be found (Zhang *et al.*, 2009a; Xue *et al.*, 2014a).

O_3 was measured using an ultraviolet photometric instrument (*Thermo Environmental Instruments (TEI)*, Model 49C). CO was measured with a modified gas filter correlation, non-dispersive infrared analyzer (*TEI*, Model 48). NO_y was measured by using a commercial chemiluminescence analyzer (*Teledyne API*, Model T200U) coupled with an outside placed molybdenum oxide (MoO) converter. NO and NO_2 were measured by a chemiluminescence analyzer (*TEI*, Model
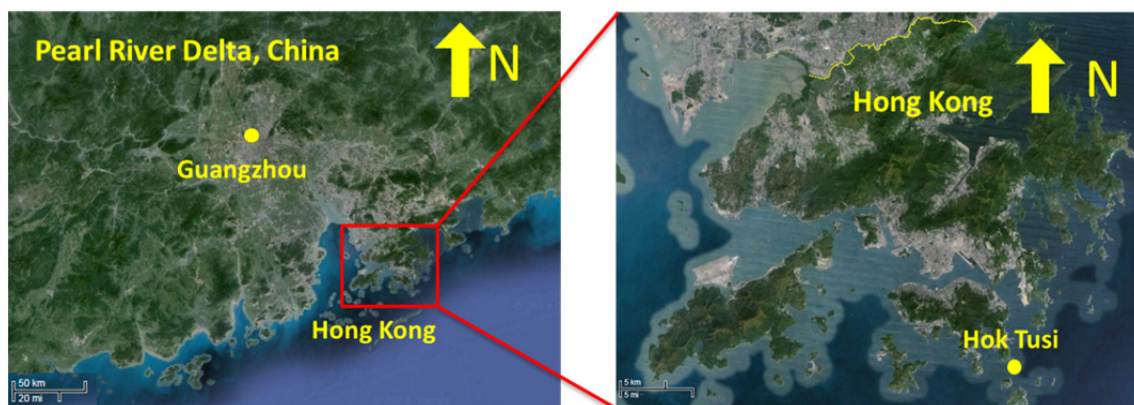

Fig. 1. Map from Google Earth showing the study region and measurement site.

42i) coupled with a highly selective photolytic converter (*Droplet Measurement Technologies*, Model Blue Light Converter) (Xu *et al.*, 2013). C_2-C_{10} NMHCs were measured with a commercial instrument combining GC separation, flame ionization detection and photoionization detection (*Syntech Spectras*, Model GC955 Series 600/800 POCP). Total non-methane hydrocarbons were measured by a back-flush GC system (*TEI*, Model 55i). Temperature, relative humidity (RH), and wind speed and direction were monitored by a commercial probe (*M. R. Young*, Model 41382VC/VF) and a two-axis ultrasonic wind sensor (*Gill Instruments*, Model 1405-PK-021). The time frequencies of measurements were 10 minutes for PAN, 30 minutes for NMHCs, and 1 minute for other parameters. In addition, acetaldehyde was measured at a 24-hour frequency on selected days by collecting air samples in 2,4-DNPH-coated sorbent cartridge with subsequent high-pressure liquid chromatography detection (Xue *et al.*, 2014a). Detailed descriptions of these measurements can be found in our previous studies (Wang *et al.*, 2001; Wang *et al.*, 2003a).

RESULTS AND DISCUSSION

Data Overview

Fig. 2 depicts the temporal variations in trace gases and meteorological parameters observed at Hok Tsui. The measurement period covered two seasons, i.e., late summer (19th August–16th September) and later autumn (9th November–5th December). A clear seasonal variation in the meteorological and pollution conditions is illustrated. In summer, diverse surface winds (both southerly and northerly) and higher temperature (and RH to a lesser extent) were recorded. The concentrations of PAN and other species were at a relatively low level during the majority of time, due to the southerly marine inflow and/or high temperatures (for

PAN). A multi-day photochemical episode occurred during 25th–31st August 2011 when Hong Kong was under the influence of a distant tropical cyclone. Northerly winds brought polluted plumes from the PRD region, which coupled with the stagnant weather conditions contributed to the maximum pollution (i.e., 4.96 ppbv and 189 ppbv of 10-minute PAN and O_3) observed during both campaigns. In comparison, strong northeasterly winds clearly dominated throughout the autumn phase, corresponding to the continental outflow to the measurement site. As a consequence, the overall pollution levels in autumn were higher than those in summer except for the typhoon-related episodes. Such a seasonal pattern is believed to be driven by the Asian Monsoons.

To make the results in a quantitative perspective, statistics of PAN and related species were calculated and summarized in Table 1. The average concentrations of PAN, NO_y, CO and O_3 were 0.48 (±0.69; standard deviation) ppbv, 10.3 (±9.8) ppbv, 191 (±141) ppbv and 33 (±25) ppbv in summer, and were 0.69 (±0.46) ppbv, 8.8 (±6.5) ppbv, 311 (±140) ppbv and 46 (±19) ppbv in autumn. Ten days were noticed with the peak 10-minute data of PAN exceeding 2 ppbv, and five days with the maximum PAN over 3 ppbv. The maximum values of PAN and O_3 were recorded at 4.96 ppbv and 189 ppbv during the afternoon of 31st August 2011. Overall, the results indicated fairly low levels of pollution in general as well as severe pollution episodes under unfavorable conditions (e.g., typhoon) at this regional background site.

Statistics on selected VOC species that are major precursors of PAN are also provided in Table 1. The average mixing ratios (± SD) of propene, toluene, m/p-xylene, o-xylene and acetaldehyde were 0.45 (± 0.29), 0.95 (± 1.08), 0.48 (± 0.67), 0.27 (± 0.39) and 1.07 (± 1.07) ppbv in summer, and 0.22 (± 0.14), 1.11 (± 1.13), 0.21 (± 0.69), 0.11 (± 0.12) and 1.27 (± 0.42) ppbv in autumn. The fairly low levels are
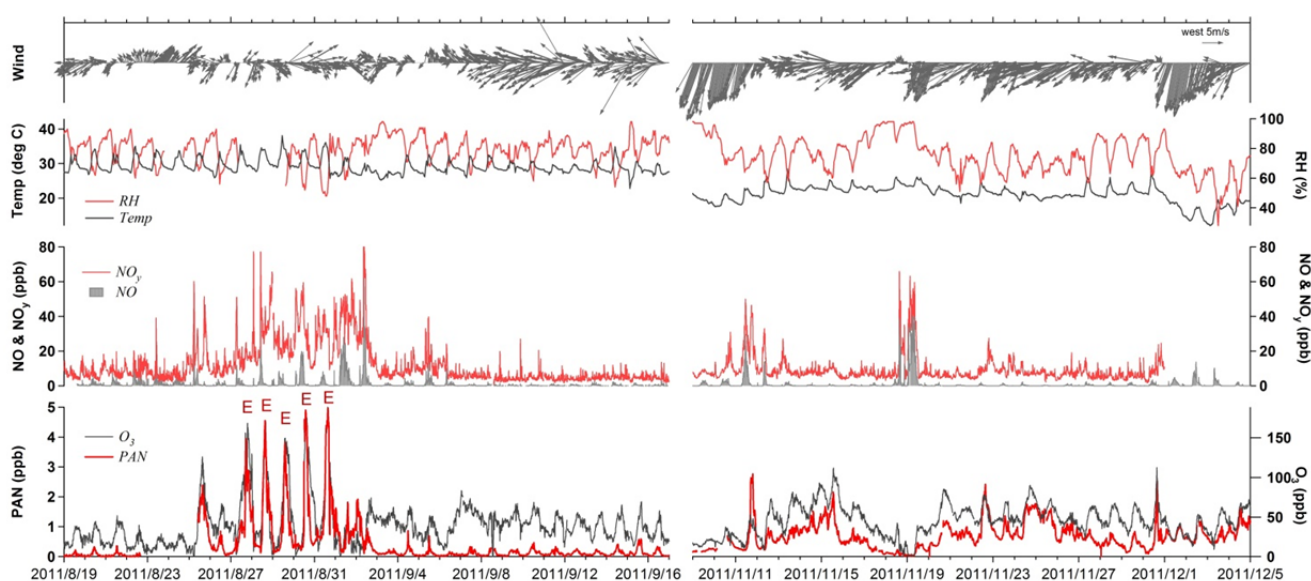

Fig. 2. Time series of trace gases and meteorological parameters observed at Hok Tsui during August 19th–September 16th and November 9th–December 5th, 2011. The character "E" indicates the episodes with the peak PAN concentration exceeding 3 ppbv.

Table 1. Statistical summary of 10-minute measurement data at Hok Tsui.

	Late summer				Late autumn			
	Average	SD	Max	Min	Average	SD	Max	Min
PAN	0.48	0.69	4.96	-	0.69	0.46	2.80	-
NO_y	10.3	9.8	119	0.6	8.8	6.5	65.9	1.7
CO	191	141	1109	-	311	140	841	71
O_3	33	25	189	2	46	19	113	2
ethane	1.64	1.31	7.59	0.40	3.31	1.45	9.60	0.83
propene	0.45	0.29	3.19	0.06	0.22	0.14	1.11	0.05
toluene	0.95	1.08	7.03	-	1.11	1.13	11.2	0.05
o-xylene	0.27	0.39	3.97	-	0.11	0.12	0.83	-
m/p-xylene	0.48	0.67	7.77	-	0.21	0.29	2.08	-
CH_3CHO	1.07	1.07	2.60	0.19	1.27	0.42	2.01	0.69

The units are ppbv. SD is standard deviation; "-" means that the data is below detection limit.

in consistence with the regional background nature of the study site. Air masses arriving at Hok Tsui either had been less influenced by fresh anthropogenic emissions or had undergone photochemical processing. An interesting result is that the aromatic precursors were generally more abundant than the alkene precursors, implying that the aromatics may play an important role in PAN formation in Hong Kong.

Fig. 3 presents the average diurnal variations of PAN, O_3, CO, NO and NO_y observed at Hok Tsui. CO and NO showed the maximum concentrations in the morning, reflecting advection of fresh urban plumes to the study site. NO_y showed a coincident concentration peak in the morning period, with a secondary peak in the evening. O_3 presented a typical diurnal pattern characteristic of rural atmosphere, with the mixing ratios increasing from early morning (07:00 local time (LT)) to late afternoon (15:00 LT). The average daily O_3 increment was approximately 30 ppbv, indicating fair photochemical ozone production at this regional background station.

PAN exhibited a well-defined diurnal pattern, similar to that of O_3, with relatively stable lower concentrations at night and a clear increase during the daytime. The daytime increment of PAN was about 0.52 ppbv on average. The highest concentrations occurred at 14:00–15:00 LT (~0.90 ppbv), when the solar radiation was the most intensive and thus the photochemistry was the most active. At its maximum, PAN accounted for approximately 10% of NO_y and 25% of NO_z. After that, PAN began to decline due to the gradually weakened photochemistry and continuous thermal decomposition, and reached its minimum (~0.40 ppbv) till the night. Also shown in Fig. 3 are the individual diurnal profiles of PAN in both summer and fall. PAN showed comparable maximum concentrations in the afternoon but distinct levels at nighttime in both seasons. The nighttime levels (~0.15 ppbv) in summer were much lower than those observed in autumn (~0.47 ppbv), which should be due to the import of marine air masses as well as faster thermal decomposition at higher temperatures in summer. On the other hand, the daytime increment was much larger in summer (~0.74 ppbv) than in autumn (~0.35 ppbv), indicating stronger photochemical production of PAN in summer. Overall, inspection of the diurnal profiles reveals the important roles of photochemical production and transport in the variations of PAN (and other pollutants).

Production Efficiency of O_3 and PAN

Although PAN and O_3 are co-products of photochemistry involving NO_x and VOCs, they have different production efficiencies. This is because PAN is only formed from certain kinds of VOCs that are precursors of the acetyl radical (CH_3CO), while O_3 can be produced from oxidation processes of all VOCs (Grosjean *et al.*, 2002). Correlation between PAN and O_3 can provide some useful information on their photochemical production efficiencies. An excellent positive correlation between the daily maximum values of PAN and O_3 at Hok Tsui is shown in Fig. 4 ($r^2 = 0.82$). The slope of linear regression is 0.028 ppbv/ppbv, which indicates that approximately 2.8 ppbv of PAN could be produced on average during the formation of 100 ppbv of O_3 in the air masses reaching Hok Tsui. This value is comparable to those determined at Back Garden, a rural site in the PRD region (0.015–0.028 ppbv/ppbv, Wang *et al.*, 2010a), Nashville (0.025 ppbv/ppbv, Roberts *et al.*, 2002), and Mexico City (0.02 ppbv/ppbv, Marley *et al.*, 2007), but much lower than those obtained in Lanzhou (0.091 ppbv/ppbv, Zhang *et al.*, 2009a) and Beijing (0.07 ppbv/ppbv, Zhang *et al.*, 2011). This relatively low production efficiency of PAN with respect to O_3 implies that PAN precursors only made a small fraction of the total VOCs in the upwind regions. Indeed, the sum concentration of the observed PAN precursors (see Table 1) only accounted for about 20% of the total VOCs at Hok Tsui. Another factor leading to the lower production efficiency of PAN should be the high temperature in the PRD region that facilitates thermal decomposition of PAN.

We further assessed the production efficiencies of O_3 and PAN during the photochemical episodes with the peak PAN value exceeding 3 ppbv (27th–31st August 2011; see Fig. 2). Backward trajectories suggested that the plumes sampled at Hok Tsui were mainly originated from the PRD under influence of a tropical cyclone (figures not shown), and hence the results should be representative of the PRD region. Fig. 5 presents the strong positive correlations between simultaneous data of PAN versus O_3 on the individual episode days ($r^2 = 0.71$–0.99). The slopes of $\Delta PAN/\Delta O_3$ were in the range of 0.013–0.031 ppbv/ppbv, with a 'mean' value (i.e., slope of correlation for all data) of 0.029 ppbv/ppbv.

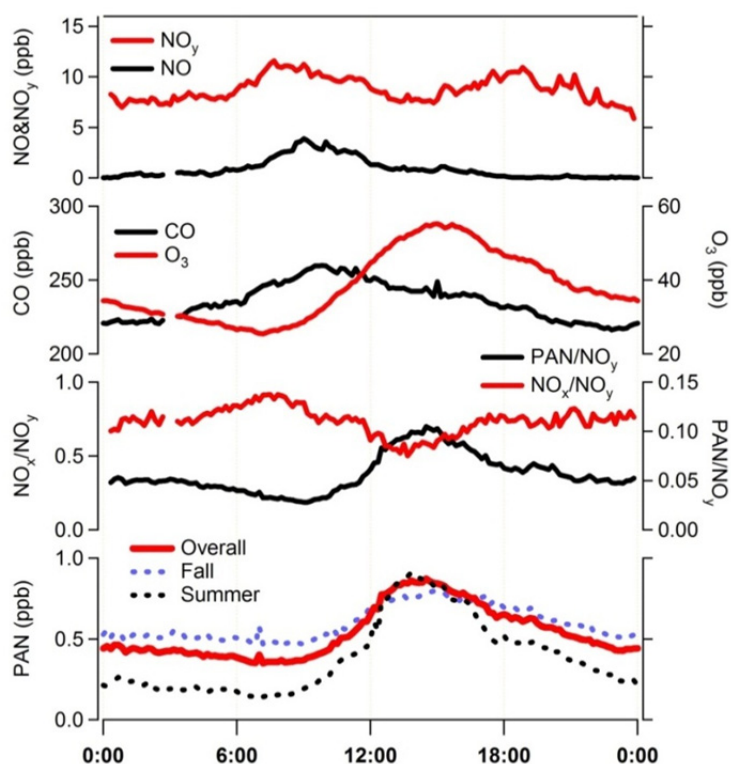**Fig. 3.** Average diurnal variations of PAN, O_3, NO, NO_y, PAN/NO_y, and NO_x/NO_y observed at Hok Tsui. The individual profiles in summer and fall are also shown for PAN.
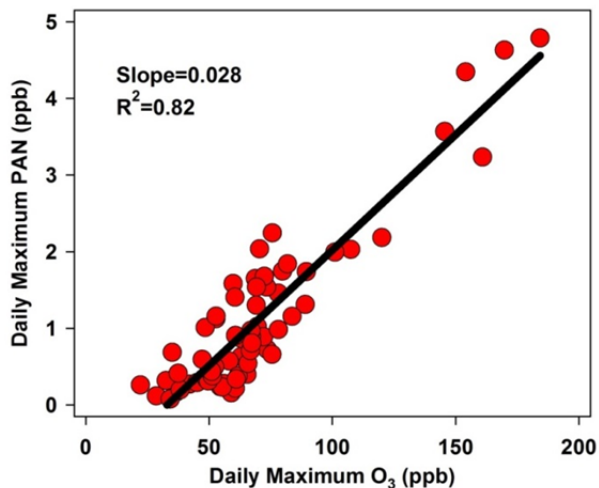

Fig. 4. Scatterplot of the daily maximum PAN versus daily maximum O_3 observed at Hot Tsui.

These values agreed well with that derived from analysis of daily maximums (Fig. 4). Comparison with other studies suggests that the production efficiency of PAN in the PRD region seemed to be relatively lower than those in Beijing and Lanzhou (Zhang *et al.*, 2009a; Zhang *et al.*, 2011).

Ozone production efficiency (OPE) is usually defined as the number of O_3 molecules produced per each NO_x molecule oxidized, and is determined as the slope of scatterplots of O_3 versus NO_z (Trainer *et al.*, 1993; Wang *et al.*, 2010b). In the present study, OPE values of 9.0–13.3 were derived

for the individual episode days based on correlation analyses of daytime measurements (08:00–17:00 LT) of O_3 and NO_z (see Fig. 6(a)). These high values suggest that photochemical ozone production at Hok Tsui was in a NO_x-limited regime, which is in line with the rural nature of the atmosphere.

In the present study, we adopt a similar approach to estimate the PAN production efficiency (PPE), which is defined as the amount of PAN formed per unit amount of NO_x oxidized. Similarly, it is calculated as the slope of the scatterplot of PAN versus NO_z, and can provide useful information on the fraction of PAN production to the total NO_x oxidation. PPE (i.e., $\Delta PAN/\Delta NO_z$) is a better proxy of the fraction of NO_z produced in the form of PAN than the PAN/NO_z ratio, which is generally influenced by the different lifetimes between PAN and other NO_z species. Fig. 6(b) shows the scatterplots of daytime (08:00–17:00 LT) data of PAN and NO_z during the photochemical episodes. The derived PPE values were in the range of 0.17–0.38 ppbv/ppbv, with a 'mean' value (i.e., the slope of correlation for all data) of 0.32 ppbv/ppbv. This indicates that on average only 32% of NO_2 were converted to PAN while the rest was oxidized to other forms of NO_z such as nitric acid, inorganic nitrate, and other organic nitrates. These results provide useful insights into the NO_x oxidation and NO_z budget in the PRD plumes.

Impact of Regional Transport

To evaluate the influence of regional transport on the observed PAN levels, we classified all the air masses into several major groups based on cluster analysis of backward
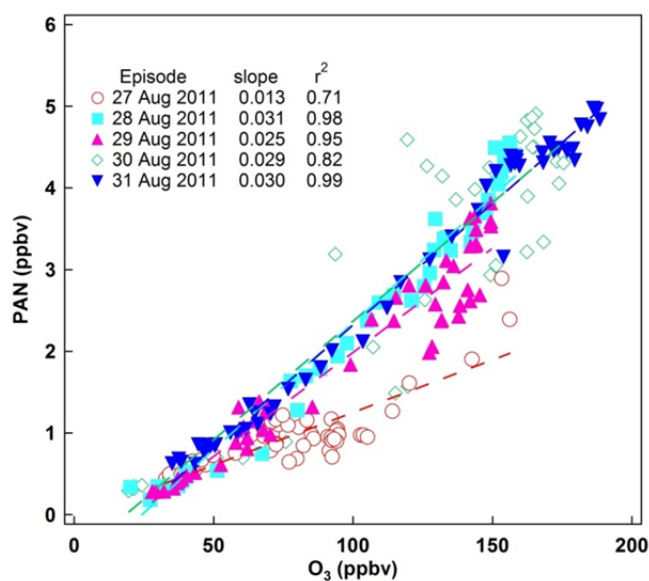
Fig. 5. Scatter plots of PAN versus O_3 during the selected photochemical episodes. The 10-min data at daytime (08:00–17:00, LT) are used.
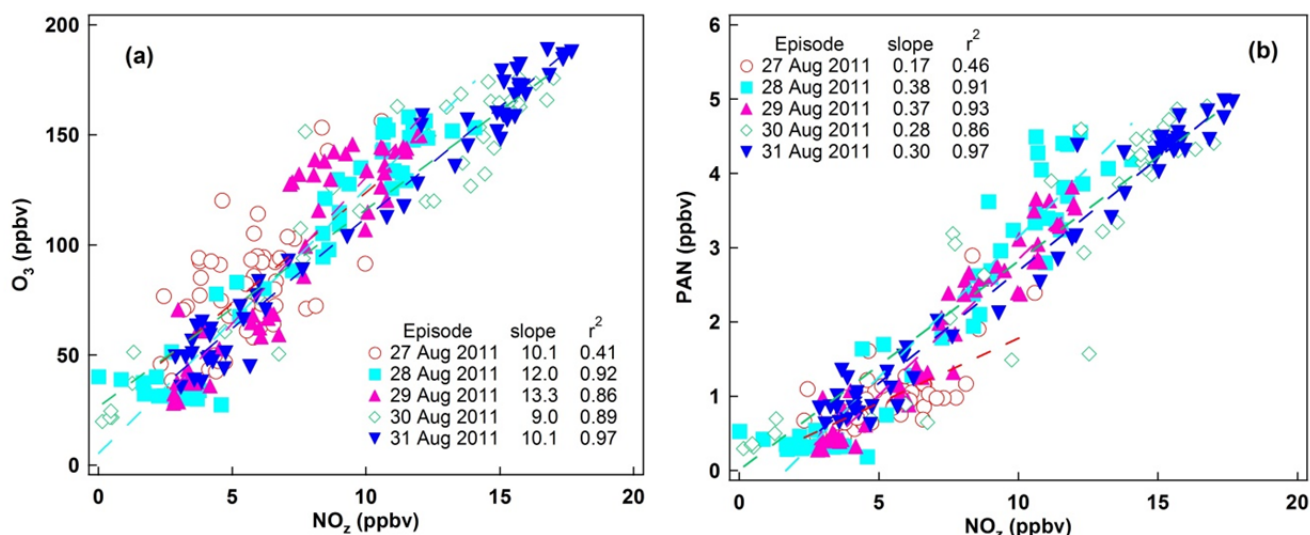

Fig. 6. Scatter plots of (a) O_3 versus NO_z and (b) PAN versus NO_z during the selected photochemical episodes. The 10-min data at daytime (08:00–17:00, LT) are used.

trajectories. Three-day backward trajectories were calculated with the HYSPLIT model every hour during the measurement campaigns, and were then identified to four different groups with a cluster analysis approach (Wang *et al.*, 2009). The average trajectories representative of the four air mass types are shown in Fig. 7. The four types were referred to here as "East China" "Marine", "PRD", and "Central China + PRD", the name of which suggests the origins and regions over which the air masses had passed. Throughout the measurement period, the "East China" group occurred the most (36% in percentage), followed by "PRD" (24%), "Marine" (24%) and "Central China + PRD" (16%). The transport pattern derived from the present study in summer and autumn of 2011 was consistent with the climatological one determined for the years of 1994–2007 at the same site

by Wang *et al.* (2009)

In addition, we also examined the CO/NO_y ratios to confirm the identification of air mass origins from the trajectory analyses. According to Wang *et al.* (2003b), air masses originating from Hong Kong usually had a relatively lower CO/NO_y ratio (i.e. 3.9–6 ppbv/ppbv); the PRD regional air masses contained a much larger one (i.e., ~20 ppb/ppb); and the ratio in the aged air masses from eastern China was even much higher (near to 40, Wang *et al.*, 2004; Li *et al.*, 2007). The difference in the CO/NO_y ratio should be ascribed to the difference in energy consumption and air mass ages (note that CO has a longer lifetime than NO_y thus the ratio increases with the air mass aging). In the present study, the average CO/NO_y ratio of the "PRD" air masses was calculated as 18.2 ppb/ppb, while those of the "East China" and "Central
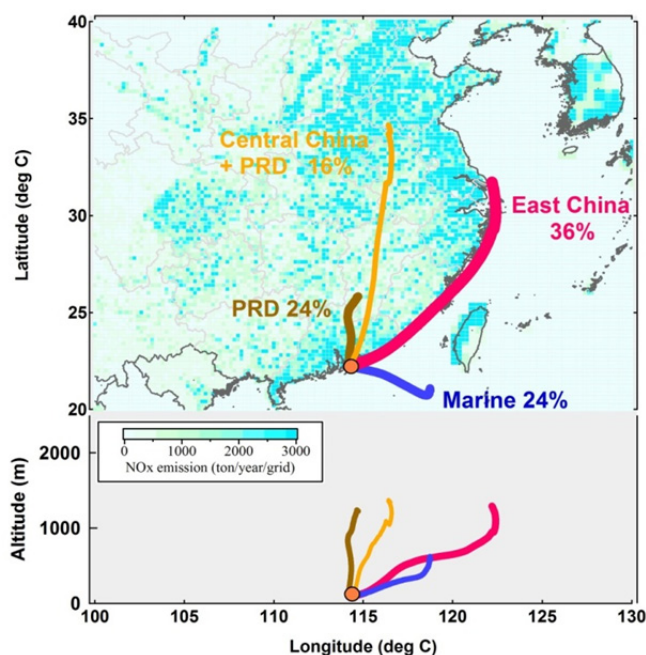
Fig. 7. Four major types of 3-day backward trajectory arriving at Hok Tsui during the observation periods. The percentage of each type is also given. The anthropogenic NO_x emission data is obtained from Zhang *et al.* (2009b).

Table 2. Chemical characteristics of the four types of air masses arriving at Hok Tsui.

Air mass type	PAN (*ppb*)	NO_x (*ppb*)	NO_y (*ppb*)	CO (*ppb*)	O_3 (*ppb*)	TNMHC (*ppm*)	NO_x/NO_y	CO/NO_y	PAN/NO_z	Temp (°C)
Marine	0.15	5.4	7.5	128	32	0.011	0.73	17.1	0.07	28
PRD	0.86	16.4	19.5	355	50	0.046	0.84	18.2	0.31	26
East China	0.62	3.0	5.9	276	51	0.013	0.50	46.7	0.17	24
Central China + PRD	0.61	8.7	10.1	412	35	0.038	0.86	40.9	0.34	21

China + PRD" were 46.7 ppb/ppb and 40.9 ppb/ppb, respectively (see Table 2). These results agree well with the previous studies and hence double validate the classification of different air masses.

Table 2 summarizes the average concentrations of PAN, O_3, CO, NO_x, NO_y, total NMHCs and ratios of NO_x/NO_y, CO/NO_y and PAN/NO_z for the four types of air masses. The "Marine" air masses showed the lowest levels of PAN (0.15 ppbv) and other species as well. Note that the NO_x and NO_y levels in the "Marine" group were relatively higher than those in the "East China" group. This should be due to the occasional impact of fresh ship emissions, which is supported by the high ratio of NO_x/NO_y (0.73). In comparison, the highest levels of PAN (0.87 ppbv) and other pollutants were found in the "PRD" air masses. This was within the expectation in light of the intense anthropogenic emissions in the PRD region as well as the relatively short transport time to the measurement site. The "East China" and "Central China + PRD" groups contained comparable abundances of PAN (0.62 and 0.61 ppbv), but showed different profiles for the other species. Specifically, the more aged "East China" air masses had higher levels of O_3 but lower concentrations of O_3 (also PAN) precursors (i.e., NO_x, CO and NMHCs), while an opposite pattern was found for the "Central China + PRD" group that may be influenced by

fresh emissions in the PRD.

Also illustrated from Table 2 are the varying PAN/NO_z ratios reflecting different NO_z composition in different air masses. On average, PAN accounted for 31% and 34% of the NO_z in the air masses of "PRD" and "Central China + PRD". These values were consistent with the PAN production efficiency determined for the photochemical episodes (see Fig. 6(b)). In comparison, the "East China" air mass group showed a relatively lower ratio of 0.17, implying the predominant role of inorganic nitrates in the NO_z compounds. The lowest PAN/NO_z ratio (0.07) was found in the "Marine" air masses, which are believed to contain large amount of sea salt that is conductive to the production of inorganic nitrates. Overall, the above analyses highlight the significant role of regional transport in the ambient abundances of PAN and related pollutants in Hong Kong. The chemical signatures determined in the present study can be used for future studies to infer the origins of different air masses. The concentration of PAN in the "Marine" air masses could serve as the regional background value of southern China.

CONCLUSIONS

Intensive measurements were performed at Hok Tsui in the summer and autumn of 2011 to understand the chemical

and transport processes of PAN in the PRD region. The ambient concentrations of PAN and PAN precursors were fairly low at this rural site, with relatively higher levels in autumn than in summer. Severe photochemical episodes were observed under unfavorable conditions (i.e., typhoon-influenced) with the PAN and O_3 mixing ratios up to 4.96 and 189 ppbv. Different air masses including oceanic air, regional plumes from the PRD, and continental outflow from eastern China, were sampled during the measurement period, which showed distinct chemical signatures. The highest levels of PAN and other pollutants were found in the PRD regional plumes, whilst the lowest levels were measured in the oceanic air.

The photochemical production efficiencies of PAN and O_3 as well as NO_z budget were examined in the polluted plumes from the PRD. The ozone production efficiency was in the range of 9.0–13.3 ppbv/ppbv, indicating that the local O_3 production was in a NO_x-limited regime. The average PAN production efficiency was 0.32 ppbv/ppbv, indicating that about one third of the NO_z was produced in the form of PAN in the PRD air masses. According to correlation analyses between PAN and O_3, about 2.9 ppbv of PAN was produced on average when 100 ppbv of O_3 was formed. The production efficiency of PAN with respect to O_3 in the PRD region was much lower than those determined in Beijing and Lanzhou, China. This study can provide useful information on the photochemical production and regional transport of PAN in the PRD region.

ACKNOWLEDGEMENTS

DISCLAIMER

The opinions expressed in this paper are those of the authors and do not necessarily reflect the views or policies of the Government of Hong Kong Special Administrative Region, nor does any mention of trade names or commercial products constitute an endorsement or recommendation of their use.

REFERENCES

Aneja, V.P., Hartsell, B.E., Kim, D.S. and Grosjean, D. (1999). Peroxyacetyl Nitrate in Atlanta, Georgia: Comparison and Analysis of Ambient Data for Suburban and Downtown Locations. *J. Air Waste Manage. Assoc.* 49: 177–184.

Ding, A., Wang, T., Zhao, M., Wang, T. and Li, Z. (2004). Simulation of Sea-land Breezes and a Discussion of Their Implications on the Transport of Air Pollution during a Multi-day ozone Episode in the Pearl River Delta of China. *Atmos. Environ.* 38: 6737–6750.

Gaffney, J.S., Marley, N.A., Cunningham, M.M. and Doskey, P.V. (1999). Measurements of Peroxyacyl Nitrates (PANS) in Mexico City: Implications for Megacity Air Quality Impacts on Regional Scales. *Atmos. Environ.* 33: 5003–5012.

Grosjean, D. (2003). Ambient PAN and PPN in Southern California from 1960 to the SCOS97-NARSTO. *Atmos. Environ.* 37: 221–238.

Grosjean, E., Grosjean, D., Woodhouse, L.F. and Yang, Y.J. (2002). Peroxyacetyl Nitrate and Peroxypropionyl Nitrate in Porto Alegre, Brazil. *Atmos. Environ.* 36: 2405–2419.

LaFranchi, B., Wolfe, G., Thornton, J., Harrold, S., Browne, E., Min, K., Wooldridge, P., Gilman, J., Kuster, W. and Goldan, P. (2009). Closing the Peroxy Acetyl Nitrate Budget: Observations of Acyl Peroxy Nitrates (PAN, PPN, and MPAN) during BEARPEX 2007. *Atmos. Chem. Phys.* 9, 7623–7641.

Li, C., Marufu, L.T., Dickerson, R.R., Li, Z., Wen, T., Wang, Y., Wang, P., Chen, H. and Stehr, J.W. (2007). In Situ Measurements of Trace Gases and Aerosol Optical Properties at a Rural Site in northern China during East Asian Study of Tropospheric Aerosols: An International Regional Experiment 2005. *J. Geophys. Res.* 112, D22S04.

Ling, Z.H., Guo, H., Lam, S.H.M., Saunders, S.M. and Wang, T. (2014). Atmospheric Photochemical Reactivity and Ozone Production at Two Sites in Hong Kong: Application of a Master Chemical Mechanism–Photochemical Box Model. *J. Geophys. Res.* 119: 10567–10582.

Liu, Z., Wang, Y., Gu, D., Zhao, C., Huey, L.G., Stickel, R., Liao, J., Shao, M., Zhu, T., Zeng, L., Liu, S.C., Chang, C.C., Amoroso, A. and Costabile, F. (2010). Evidence of Reactive Aromatics As a Major Source of Peroxy Acetyl Nitrate over China. *Environ. Sci. Technol.* 44: 7017–7022.

Marley, N., Gaffney, J., Ramos-Villegas, R. and Cárdenas González, B. (2007). Comparison of Measurements of Peroxyacyl Nitrates and Primary Carbonaceous Aerosol Concentrations in Mexico City Determined in 1997 and 2003. *Atmos. Chem. Phys.* 7: 2277–2285.

Penkett, S.A. and Brice, K.A. (1986). The Spring Maximum in Photo-oxidants in the Northern Hemisphere Troposphere. *Nature* 319: 655–657.

Roberts, J.M., Flocke, F., Stroud, C.A., Hereid, D., Williams, E., Fehsenfeld, F., Brune, W., Martinez, M. and Harder, H. (2002). Ground-based Measurements of Peroxycarboxylic Nitric Anhydrides (PANs) during the 1999 Southern Oxidants Study Nashville Intensive. *J. Geophys. Res.* 107: ACH 1–1-ACH 1-10.

Rubio, M.A., Oyola, P., Gramsch, E., Lissi, E., Pizarro, J. and Downtown Santiago, Chile. *Atmos. Environ.* 38: 4931–4939.

Schrimpf, W., Müller, K., Johnen, F., Lienaerts, K. and Rudolph, J. (1995). An Optimized Method for Airborne Peroxyacetyl Nitrate (PAN) Measurements. *J. Atmos. Chem.* 22: 303–317.

Singh, H.B. and Hanst, P.L. (1981). Peroxyacetyl Nitrate (PAN) in the Unpolluted Atmosphere: An Important Reservoir for Nitrogen Oxides. *Geophys. Res. Lett.* 8: 941–944.

Singh, H.B. and Salas, L.J. (1983). Peroxyacetyl Nitrate in the Free Troposphere. *Nature* 302: 326–328.

Singh, H.B., Salas, L.J. and Viezee, W. (1986). Global Distribution of Peroxyacetyl Nitrate. *Nature* 321: 588–591.

Stephens, E.R. (1969). *The Formation, Reactions, and Properties of Peroxyacyl Nitrates (PANs) in Photochemical Air Pollution*. Wiley.

Trainer, M., Parrish, D.D., Buhr, M.P., Norton, R.B., Fehsenfeld, F.C., Anlauf, K.G., Bottenheim, J.W., Tang, Y.Z., Wiebe, H.A., Roberts, J.M., Tanner, R.L., Newman, L., Bowersox, V.C., Meagher, J.F., Olszyna, K.J., Rodgers, M.O., Wang, T., Berresheim, H., Demerjian, K.L. and Roychowdhury, U.K. (1993). Correlation of Ozone with NO_y in Photochemically Aged Air. *J. Geophys. Res.* 98: 2917–2925.

Wang, B., Shao, M., Roberts, J.M., Yang, G., Yang, F., Hu, M., Zeng, L., Zhang, Y. and Zhang, J. (2010a). Ground-based On-line Measurements of Peroxyacetyl Nitrate (PAN) and Peroxypropionyl Nitrate (PPN) in the Pearl River Delta, China. *Int. J. Environ. Anal. Chem.* 90: 548–559.

Wang, T., Cheung, V.T., Lam, K., Kok, G. and Harris, J. (2001). The Characteristics of Ozone and Related Compounds in the Boundary Layer of the South China Coast: Temporal and Vertical Variations during Autumn Season. *Atmos. Environ.* 35: 2735–2746.

Wang, T., Ding, A., Blake, D., Zahorowski, W., Poon, C. and Li, Y. (2003a). Chemical Characterization of the Boundary Layer Outflow of Air Pollution to Hong Kong during February–April 2001. *J. Geophys. Res.* 108: 8787.

Wang, T., Poon, C., Kwok, Y. and Li, Y. (2003b). Characterizing the Temporal Variability and Emission Patterns of Pollution Plumes in the Pearl River Delta of China. *Atmos. Environ.* 37: 3539–3550.

Wang, T., Wong, C.H., Cheung, T.F., Blake, D.R., Arimoto, R., Baumann, K., Tang, J., Ding, G.A., Yu, X.M., Li, Y.S., Streets, D.G. and Simpson, I.J. (2004). Relationships of Trace Gases and Aerosols and the Emission Characteristics at Lin'an, a Rural Site in Eastern China, during Spring 2001. *J. Geophys. Res.* 109: D19S05.

Wang, T., Wei, X., Ding, A., Poon, C., Lam, K., Li, Y., Chan, L. and Anson, M. (2009). Increasing Surface Ozone Concentrations in the Background Atmosphere of Southern China, 1994–2007. *Atmos. Chem. Phys.* 9: 6217–6227.

Wang, T., Nie, W., Gao, J., Xue, L.K., Gao, X.M., Wang, X.F., Qiu, J., Poon, C.N., Meinardi, S., Blake, D., Wang, S.L., Ding, A.J., Chai, F.H., Zhang, Q.Z. and Wang, W.X. (2010b). Air Quality during the 2008 Beijing Olympics: Secondary Pollutants and Regional Impact. *Atmos. Chem. Phys.* 10: 7603–7615.

Xu, Z., Wang, T., Xue, L.K., Louie, P.K.K., Luk, C.W.Y., Gao, J., Wang, S.L., Chai, F.H. and Wang, W.X. (2013). Evaluating the Uncertainties of Thermal Catalytic Conversion in Measuring Atmospheric Nitrogen Dioxide at Four Differently Polluted Sites in China. *Atmos. Environ.* 76: 221–226.

Xue, L.K., Wang, T., Wang, X., Blake, D.R., Gao, J., Nie, W., Gao, R., Gao, X., Xu, Z., Ding, A., Huang, Y., Lee, S., Chen, Y., Wang, S., Chai, F., Zhang, Q. and Wang, W. (2014a). On the Use of an Explicit Chemical Mechanism to Dissect Peroxy Acetyl Nitrate Formation. *Environ. Pollut.* 195: 39–47.

Xue, L.K., Wang, T., Gao, J., Ding, A.J., Zhou, X.H., Blake, D.R., Wang, X.F., Saunders, S.M., Fan, S.J., Zuo, H.C., Zhang, Q.Z. and Wang, W.X. (2014b). Ground-level Ozone in Four Chinese Cities: Precursors, Regional Transport and Heterogeneous Processes. *Atmos. Chem. Phys. Discuss.* 14: 20767–20803.

Xue, L.K., Wang, T., Louie, P.K.K., Luk, C.W.Y., Blake, D.R. and Xu, Z. (2014c). Increasing External Effects Negate Local Efforts to Control Ozone Air Pollution: A Case Study of Hong Kong and Implications for Other Chinese Cities. *Environ. Sci. Technol.* 48: 10769–10775.

Zhang, J., Wang, T., Chameides, W.L., Cardelino, C., Kwok, J., Blake, D.R., Ding, A. and So, K.L. (2007). Ozone Production and Hydrocarbon Reactivity in Hong Kong, Southern China. *Atmos. Chem. Phys.* 7: 557–573.

Zhang, J., Wang, T., Ding, A., Zhou, X., Xue, L., Poon, C., Wu, W., Gao, J., Zuo, H. and Chen, J. (2009a). Continuous Measurement of Peroxyacetyl Nitrate (PAN) in Suburban and Remote Areas of Western China. *Atmos. Environ.* 43: 228–237.

Zhang, J., Xu, Z., Yang, G. and Wang, B. (2011). Peroxyacetyl Nitrate (PAN) and Peroxypropionyl Nitrate (PPN) in Urban and Suburban Atmospheres of Beijing, China. *Atmos. Chem. Phys. Discuss.* 11: 8173–8206.

Zhang, Q., Streets, D.G., Carmichael, G.R., He, K.B., Huo, H., Kannari, A., Klimont, Z., Park, I.S., Reddy, S., Fu, J.S., Chen, D., Duan, L., Lei, Y., Wang, L.T. and Yao, Z.L. (2009b). Asian Emissions in 2006 for the NASA INTEX-B Mission. *Atmos. Chem. Phys.* 9: 5131–5153.

Zhang, Y., Hu, M., Zhong, L., Wiedensohler, A., Liu, S., Andreae, M., Wang, W. and Fan, S. (2008). Regional Integrated Experiments on Air Quality over Pearl River Delta 2004 (PRIDE-PRD2004): Overview. *Atmos. Environ.* 42: 6157–6173.

Zhang, Y., Wang, X., Blake, D.R., Li, L., Zhang, Z., Wang, S., Guo, H., Lee, F.S.C., Gao, B., Chan, L., Wu, D. and Rowland, F.S. (2012). Aromatic Hydrocarbons as Ozone Precursors Before and After Outbreak of the 2008 Financial Crisis in the Pearl River Delta Region, South China. *J. Geophys. Res.* 117: D15306.

Zhong, L.J., Louie, P.K., Zheng, J.Y., Wai, K., Ho, J.W., Yuan, Z.B., Lau, A.K., Yue, D.L. and Zhou, Y. (2013). The Pearl River Delta Regional Air Quality Monitoring Network-Regional Collaborative Efforts on Joint Air Quality Management. *Aerosol Air Qual. Res.* 13: 1582–1597.